Closed-Loop Control of Ankle Position Using Muscle Afferent Feedback with Functional Neuromuscular Stimulation

Ken Yoshida, *Member, IEEE,* and Ken Horch,* *Member, IEEE*

Abstract— **This paper describes a closed-loop functional neuromuscular stimulation system that uses afferent neural activity from muscle spindle fibers as feedback for controlling position of the ankle joint. Ankle extension against a load was effected by neural stimulation through a dual channel intrafascicular electrode of a fascicle of the tibial nerve that innervated the gastrocnemius muscle. Ankle joint angle was estimated from recordings of tibialis anterior and lateral gastrocnemius spindle fiber activity made with dual channel intrafascicular electrodes. Experiments were conducted in neurally intact anesthetized cats and in unanesthetized decerebrate cats to demonstrate the feasibility of this system. The system was able to reach and maintain a fixed target ankle position in the presence of a varying external moment ranging in magnitude between 7.3 and 22 N-cm opposing the action of the ankle extensor, as well as track a sinusoidal target ankle position up to a frequency of 1 Hz in the presence of a constant magnitude 22- or 37-N-cm external moment.**

I. Introduction

ACHIEVING functional control of paralyzed limbs and muscles through neuromuscular stimulation has been an area of active research for many years [1]–[6]. Open-loop functional neuromuscular stimulation (FNS) systems have been implemented in patients to restore motion to paralyzed limbs, largely on an experimental basis [7], [8]. With most cases of open-loop stimulation, the patient must actively use visual observation of the stimulated limb to determine its position and to provide control over functional limb motions [9], [10].

More recently, closed-loop automatic control systems using artificial force and joint angle transducers have been investigated. Such closed-loop systems have been shown to improve the controllability of the limb by automatically compensating for muscle fatigue and other unexpected perturbations [2], [3], [10], [11].

An alternative to using artificial sensors is to use the natural sensors which are already present within the body. During natural volitional control of muscles, natural sensors such as muscle spindles and Golgi tendon organs relay muscle length and tendon force information from the limb through the peripheral nervous system to the central nervous system. The peripheral nervous system, including these sensors, remains intact and active below the level of the lesion in spinal cord injury patients [9]. The use of natural sensors would eliminate the durability and cosmetic problems associated with artificial external sensors, but requires that the information be extracted from peripheral nerves. Recent work with glabrous skin mechanoreceptors using cuff electrodes has shown that sufficient information can be extracted from whole nerve recordings to compensate for slip on the cat's footpad [12]–[14]. This technique has been applied experimentally to hemiplegic patients to provide feedback to control an FNS stimulator to correct footdrop using chronic cuff electrodes implanted around the sural nerve and peroneal nerve [15] . The question remains, however, whether intrafascicular recording/stimulating techniques with greater recording selectivity than these extrafascicular techniques have additional benefits that can be exploited under a FNS application.

Previous work in our lab has shown that longitudinally oriented, intrafascicular electrodes (LIFE's) used for recording multiunit neural activity are able to reliably extract information from peripheral nerves [16], [17]. Neuromuscular stimulation with LIFE's has shown that these electrodes provide localized neuromuscular stimulation with low stimulus thresholds and charge per phase requirements [18]–[20].

One complication when recording activity from natural sensors in the presence of muscle activity and limb movement is that one must deal with electromyographic and other noise sources that can be several orders of magnitude larger than the neural signals [21]. The low stimulus amplitudes associated with activating muscles through intrafascicular neural stimulation and appropriate stimulation isolation measures minimizes stimulus artifact noise. Proper shielding of the recording site and filtering suppresses electromyographic and external noise artifacts [22].

In this study we evaluated the efficacy of using muscle spindle activity as feedback in a closed-loop FNS control scheme on both neurally intact, anaesthetized and decerebrate, unanesthetized feline models. Two basic tasks were employed: 1) a joint angle hold test with varying external loads and 2) a sinusoidal joint angle tracking test with a constant external load.

II. Methods

A closed-loop control system was built to control the ankle joint by stimulating the medial gastrocnemius muscle and by

Manuscript received August 26, 1994; revised October 12, 1995. This work was supported under grants from NIH and NIDRR. *Asterisk indicates corresponding author.*

K. Yoshida was with the Department of Bioengineering, University of Utah, Salt Lake City, UT 84112. He is now with the Division of Neuroscience, University of Alberta, Edmonton, AB T6G 2S2.

*K. Horch is with the Department of Bioengineering, 2480 MEB, University of Utah, Salt Lake City, UT 84112 USA (e-mail: k.horch@m.cc.utah.edu).

Publisher Item Identifier S 0018-9294(96)01051-8.

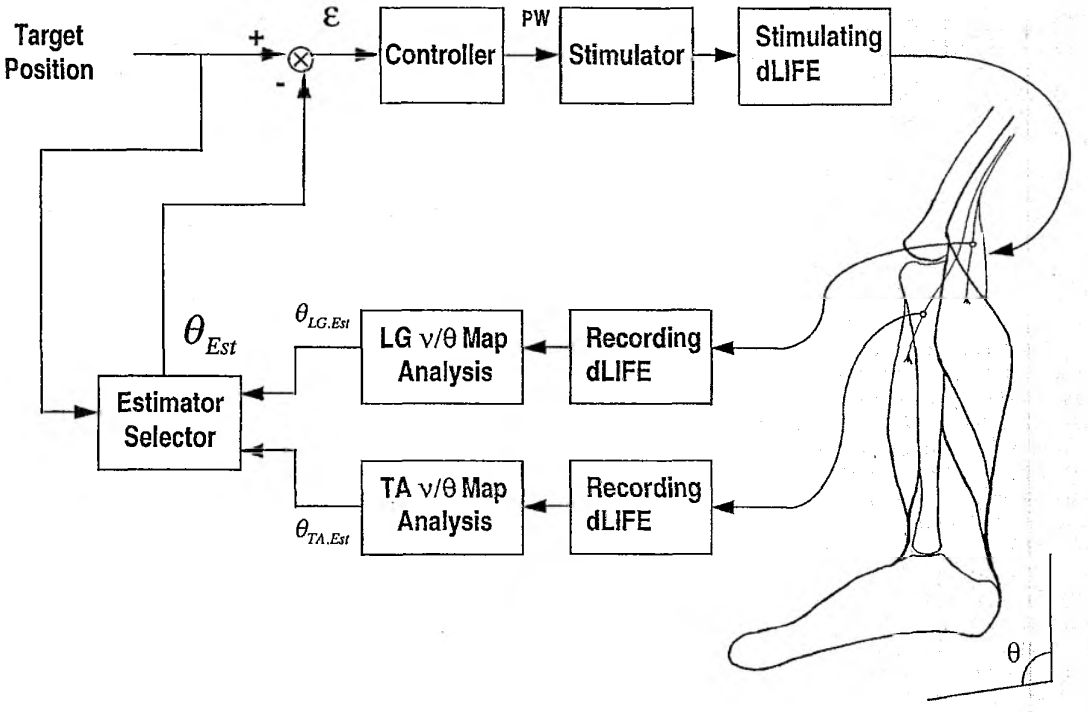

Fig. 1. Schematic system diagram. The animal preparations consisted of three dLIFE's. The stimulating dLIFE was implanted in a fascicle of the tibial nerve innervating the medial gastrocnemius muscle. The stimulus strength was modulated using pulse width modulation at a constant amplitude current pulse. A recording dLIFE was implanted within a fascicle of the common peroneal nerve innervating tibialis anterior. A second recording dLIFE was implanted within a fascicle of the tibial nerve innervating lateral gastrocnemius. The afferent activity from the muscle spindles was related to ankle joint angle through impulse frequency to joint angle ν/θ maps, and the resulting estimate of joint angle was used as feedback to the controller.

using muscle spindle activity extracted from the nerves innervating the tibialis anterior and lateral gastrocnemius muscles as feedback. A schematic diagram of this system is shown in Fig. 1. Since the purpose of this study was to assess the feasibility of using muscle spindles as a sensor in a closed-loop FNS system, rather than to build an optimized controller, *per se,* a simple PI (proportional–integral) controller was implemented to modulate the pulse width of a constant amplitude, fixed frequency stimulus pulse train. The stimulus pulse train activated the medial gastrocnemius muscle through a dual channel longitudinal intrafascicular electrode (dLIFE) implanted in an appropriate fascicle of the tibial nerve. Ankle joint position was estimated by analyzing neural activity recorded from dLIFE's implanted in the tibial and peroneal nerves. The ankle joint was loaded with an external force applied to the cat's footpad. The average moment arm for the external load about the ankle was (mean ± s.d.) 72 ± 5.8 mm. The average ankle moment arm for the medial gastrocnemius muscle was 13 ± 1.7 mm.

A. Animal Preparation

Acute experiments were conducted on 12 adult (3.8 ± 1.1 kg) cats. Ten of the cats were initially anaesthetized with an intraperitoneal injection of sodium pentobarbital (40 mg/kg), and maintained on a 1:10 dilution of the same drug administered through a catheter in the cephalic vein. To verify that anesthesia had no effect on the outcome of the experiments, two other cats were initially anaesthetized with an intramuscular injection of ketamine (10 mg/kg), intubated, and maintained on halothane while being decerebrated, after which anesthesia was discontinued. The animals were placed on a heated plate that maintained body temperature near 37.5°C. Decerebrate animals were artificially respired, with end tidal pCO_2 maintained between 23 and 30 mmHg.

The tibia in the left hind limb was anchored just above the ankle using Steinmann pins and clamps, fixing the knee at 151.3 ± 3.8° (180° = full extension). A stimulating dLIFE was implanted into single fascicles of the tibial nerve innervating medial gastrocnemius [18]–[20]. Recording dLIFE's were implanted into a single fascicle innervating lateral gastrocnemius and into the fascicle of the peroneal nerve innervating tibialis anterior. All implants were in the left leg of the cat and were performed using techniques described elsewhere [18], [23]. The fascicles to each head of the gastrocnemius muscle were visually identified by tracing the fascicles from the popliteal fossa to their insertions in the muscle. To allow visualization of the common peroneal nerve just proximal to the point where it divides into the superficial and deep branches, the insertion of the biceps femoris lateralis muscle was detached. The fascicle innervating tibialis anterior was identified using a stimulating needle electrode.

The electrodes were constructed out of 25-μm diameter Teflon® insulated 90%Pt–10%Ir wires. They consisted of two recording/stimulating electrode leads and a single indifferent electrode lead. The two recording/stimulating leads were soldered onto a single 50-μm diameter tungsten needle with the

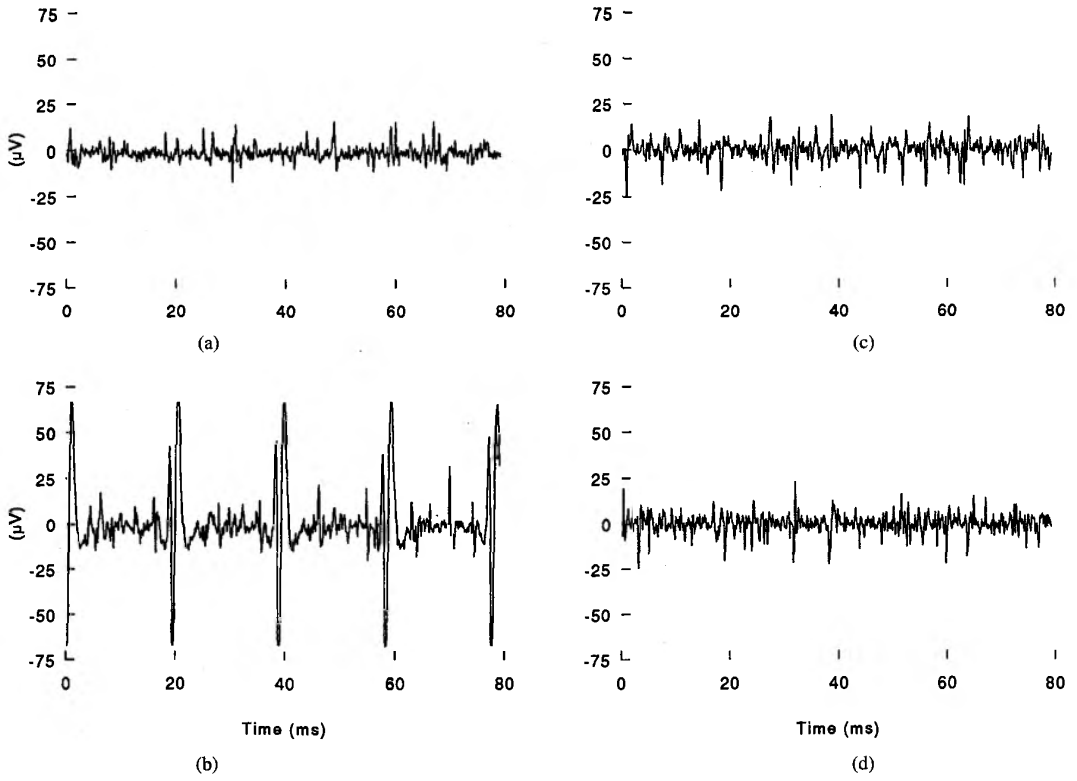

Fig. 2. Recordings from a dLIFE implanted in the peroneal nerve, with (b) and (d) and without (a) and (c), stimulation of the lateral gastrocnemius muscle. The implant site placed the active zones of the electrodes directly above the lateral head of the gastrocnemius which were shielded by wrapping the implanted fascicle with a flexible Faraday cage. Two recording methods are shown: (a) and (b) Single channel and (c) and (d) dual channel, differential. In the latter case, the electromyographic noise from the underlying muscle was almost completely suppressed. The filter (5-pole 300-Hz high pass Butterworth, 1-pole 10-kHz low pass) and gain (10 000×) settings were identical in all four cases. Activation of the muscle was effected through stimulation of a fascicle in the tibial nerve using dLIFE's and a Grass Instrument Co. stimulus isolation unit.

active regions of the two leads longitudinally displaced by 2–3 mm. The recording/stimulating leads were threaded inside a single fascicle parallel to its longitudinal axis and secured in place to the connective tissue encasing the fascicle using 9–0 suture. The wires were cut just distal to the exit point from the nerve, removing the tungsten needle and isolating the two recording/stimulating channels from each other. The indifferent electrode was secured in place outside of the fascicle adjacent to the intrafascicular pair.

B. Recording

The recording electrodes were implanted in fascicles within a few centimeters of the innervation zone of their target muscles. The resulting electromyographic noise and movement artifacts, if not suppressed, could be several orders of magnitude larger than the neural signal. Three measures were taken to suppress these artifacts: 1) a flexible Faraday cage wrapped around the nerve trunk at the level of the implant sites provided an electrical shield, 2) differential dual channel recording allowed for common mode rejection of artifacts, and 3) filtering the neural reduced the remaining noise components while allowing good resolution of neural action potentials [21].

The Faraday cage was constructed from a Kimwipe® made conductive by sputtering gold onto its surface and was placed in contact with the extrafascicular reference electrode to minimize the potential gradient imposed by external sources around the recording site. The differential recordings were made between the two intrafascicular pairs of the dLIFE using a World Precision Instruments DAM-50 differential amplifier with a gain of 10 000×. The amplifier was grounded to the extrafascicular reference electrode. Since the Faraday cage was open on two ends, residual EMG gradients could form longitudinally along the axis of the nerve. This residual EMG can be minimized by keeping the longitudinal spacing of the intrafascicular electrode pair small, and keeping the recording site centered in the Faraday cage. The unit signal amplitude, however, increases with increased longitudinal electrode spacing. An intrafascicular electrode spacing between 1 and 3 mm was used to insure reasonable signal sizes and EMG rejection. A fifth–order Butterworth high pass filter with a corner frequency of 300 Hz was used to minimize the remaining EMG, 60-Hz and 120-Hz noise. A single-pole 10-kHz low pass filter removed high frequency noise. These techniques are analogous to those described to reduce EMG artifacts in cuff electrode recordings [21], [24]. The efficacy of these techniques is illustrated in Fig. 2.

C. Joint Angle Estimation

Joint angle position information was extracted from multi-unit activity containing approximately 10 to 20 single muscle

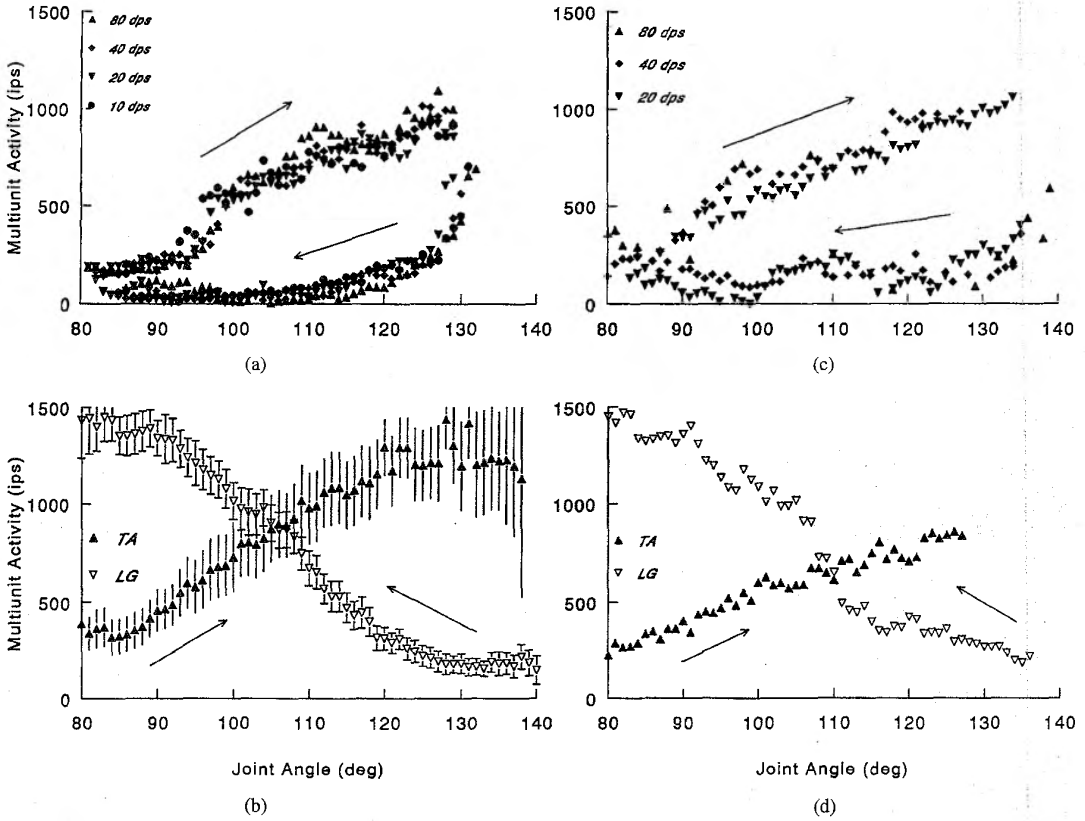

Fig. 3. Frequency (impulses per second, ips) of recorded multiunit activity as a function of ankle joint angle in (a) and (b) anesthetized ($N = 10$) and (c) and (d) unanesthetized, decerebrate ($N = 2$) preparations. The ankle joint was moved passively at the rates indicated in (a) and (c). The frequency of the recorded activity was partitioned into 1° bins over the range of joint angles studied. Bins were created separately for plantar flexion and for dorsiflexion; (a) and (c) show data from tibialis anterior in individual animals; (b) and (d) give group means for both tibialis anterior (solid symbols) and lateral gastrocnemius (open symbols). The error bars in (b) show standard errors. Arrows indicate the direction of ankle motion during data collection.

spindle units recorded in nerve fascicles innervating tibialis anterior and lateral gastrocnemius [16], [25], [26]. The background noise envelope was determined by measuring the maximum-to-peak spike amplitude with the muscle unloaded and slack. The multiunit activity was quantified using a frequency to voltage converter, with the spike acceptance threshold level set just above the envelope of the background noise. This produced a voltage that was inversely proportional to the period between successive spikes that crossed the acceptance threshold on their rising edge. This voltage representation of neural activity was sampled unfiltered with an A/D data acquisition board. We will refer to the relationship between the level of muscle spindle activity and ankle joint angle as an "activity to joint angle map." Such maps were generated by externally sweeping the ankle joint at a fixed angular velocity through the range of motion of the joint using a servocontrolled motor (Fig. 3). Firing rates were averaged into 1° bins between 80 and 140°C (180°C = full extension), and bins were created separately for plantar flexion and for dorsiflexion.

There are two characteristic responses from muscle spindles corresponding to the two types of spindle endings. The primary endings characteristically respond to the time rate of change in the length of the spindle organ whereas the secondary endings are sensitive to the length of the spindle organ. However, both endings have static length sensitivity and show increased sensitivity to phasic vibratory stretches of the spindle organ [27]. In a multiunit nerve recording the recorded activity typically reflects a mixture of the activity from these two endings, so it is influenced by rate of stretch as well as position. Under our recording and experimental conditions, stretch rates varied from 2.5 to 20 mm/s [28] and the rate effect was found to be minimal [Fig. 3(a) and (c)]. This indicates that the activity to joint angle maps were characterized using only the static sensitivity of the primary and secondary spindles, ignoring their dynamic sensitivity properties.

Spindle activity increased monotonically as the muscle was being stretched, but essentially ceased when the spindle was shortened, producing significant hysteresis when the ankle joint was cycled through its full range of motion [Fig. 3(a) and (c)]. This behavior of the spindles during muscle shortening was due to the unloading of the spindles without active fusimotor drive to take up the slack in the spindles [26]. Since this unloading of the spindles is rate limited by the viscoelastic properties of the flaccid muscle, varying the rates of muscle shortening did not significantly alter the behavior of the afferent activity.

In order to overcome the problem of hysteresis during motions that require both ankle extension and flexion, an estimation scheme using the antagonistic muscle pair of lateral

gastrocnemius and tibialis anterior was devised such that only the activity corresponding to the stretching of muscle spindles was used [Fig. 3(b) and (d)]. The direction of the required motion to achieve the target joint angle was used to select the valid estimator. For instance, if the target joint angle required the foot to move in plantar flexion, the activity from tibialis anterior was used to estimate joint position, while the activity from lateral gastrocnemius was ignored. Likewise, if the required motion was in dorsiflexion, the activity from lateral gastrocnemius was used while the activity from tibialis anterior was ignored.

The activity to joint angle maps for the unanesthetized decerebrate preparations [Fig. 3(c) and (d)] were similar to those found in the Nembutal anesthetized preparations [Fig. 3(a) and (b)]. These neural activity to joint angle maps were used by the joint angle estimator as look up tables. When using the controller, the observed impulse frequency was matched to the closest firing rate in the joint angle look up table. The corresponding joint angle was the output of the estimator and provided joint angle feedback information to the controller. In several experiments, the activity to joint angle maps generated at the beginning of the experiment were compared and found to be indistinguishable from those generated at the end of an experiment several hours later, indicating that the muscle spindle response properties were stable for the duration of the experiment.

D. Controller Implementation

A PI controller was implemented in software on a 25-MHz 386 compatible PC that modulated the duration of fixed amplitude, fixed frequency stimulus pulses between 8 and 110 μs. The controller sampling rate and the stimulus frequency were both set to 50 Hz. This rate simplified software timing while supplying a sufficiently high stimulus rate to elicit smooth fused tetanic contractions in medial gastrocnemius. It also provided a reasonable controller sampling rate within the constraints imposed by hardware. The pulse amplitude was set at a level that fully recruited medial gastrocnemius with a pulse duration near 50 μs. The average pulse amplitude (mean $\pm$ s.d.) was 49 $\pm$ 31 μA and the maximum charge per pulse was 6.0 $\pm$ 3.0 nC. The controllers were tuned to provide bounded input bounded output (BIBO) stable responses to a step change in target joint angles with the ankle loaded with a constant 3-N force at the cat's footpad. This generated a -22 ± 1.7 N-cm isotonic external moment (positive moment is defined as a moment that would generate motion in ankle extension) that opposed the action of the controlled muscle. Once these controller variables were set at the beginning of the experiment, they were kept constant throughout the remaining procedures.

To demonstrate control of the ankle joint, two tests were devised: A joint angle hold test and a joint angle trajectory tracking test. In these tests, the ankle joint was externally loaded at the foot pad through a mechanical arm linked to a servocontrolled dc motor. Ankle joint position was measured with a potentiometer coupled to the mechanical arm. A load cell mounted at the end of the mechanical arm directly measured the load force at the cat's footpad.

E. Joint Angle Hold

The joint angle hold test required the controller to deliver appropriate stimuli to the gastrocnemius muscle to maintain a specified ankle joint angle in the presence of a varying external load placed at the cat's footpad. Five target positions were evaluated: 95, 102, 110, 117, and 125°. A 125° ankle joint angle approaches the 130 $\pm$ 2° maximum physiological ankle extension during walking [29]. A 3-N external load was just sufficient to push the foot to about 95°, the minimum target position. The external load profile was comprised of two phases, each 4 s in duration. The first phase tested control in the presence of a load which varied between 1 and 3 N (-7.3 and -22 ± 1.7 N-cm). The second phase tested for muscle fatigue compensation with a constant load of 3 N. Since this test required only motions in ankle extension, the estimated joint position was derived only from the activity in tibialis anterior muscle spindles.

F. Joint Angle Trajectory Tracking

The joint angle trajectory tracking test required the controller to appropriately stimulate the gastrocnemius muscle to track a sinusoidal joint angle trajectory in the presence of a constant external load placed at the cat's footpad. Each experiment consisted of tracking repeated periods of sinusoidal trajectories for five different frequencies: 0.16, 0.31, 0.62, 1.25, and 2.50 Hz. Four different conditions of angular amplitude of the trajectory and load were tested: 35° range with a 5-N load, 35° with 3 N, 20° with 5 N, and 20° with 3 N. The maximum load of 5N (-36 ± 2.8 N-cm) was selected to be about half the maximum isometric tetanic force that the fresh muscle could produce. Since this test required motions in both ankle flexion and extension, joint position was estimated using the muscle spindle activity from both tibialis anterior and lateral gastrocnemius. The appropriate estimate was selected based upon the direction of the target trajectory. For example, if the target trajectory was toward ankle extension or was constant, spindle activity from tibialis anterior was selected. If the target trajectory was toward ankle flexion, spindle activity from lateral gastrocnemius was selected.

III. Results

A. Joint Angle Hold

The joint angle hold test was designed to test whether the controller could compensate for a varying external load and for fatigue while maintaining a constant joint position. The controller compensated for these changes to by varying the stimulus strength (Fig. 4).

Fig. 5 shows the results of the joint angle hold test from two experiments, and Fig. 6 summarizes the data from all the animals. The results were similar for anesthetized and unanesthetized decerebrate preparations (Fig. 5). On average, the controller was able to position the ankle and maintain it within 4° of the target position in the presence of a variable external load and muscle fatigue. The steady–state accuracy of the joint angle estimator was greater at small angles with

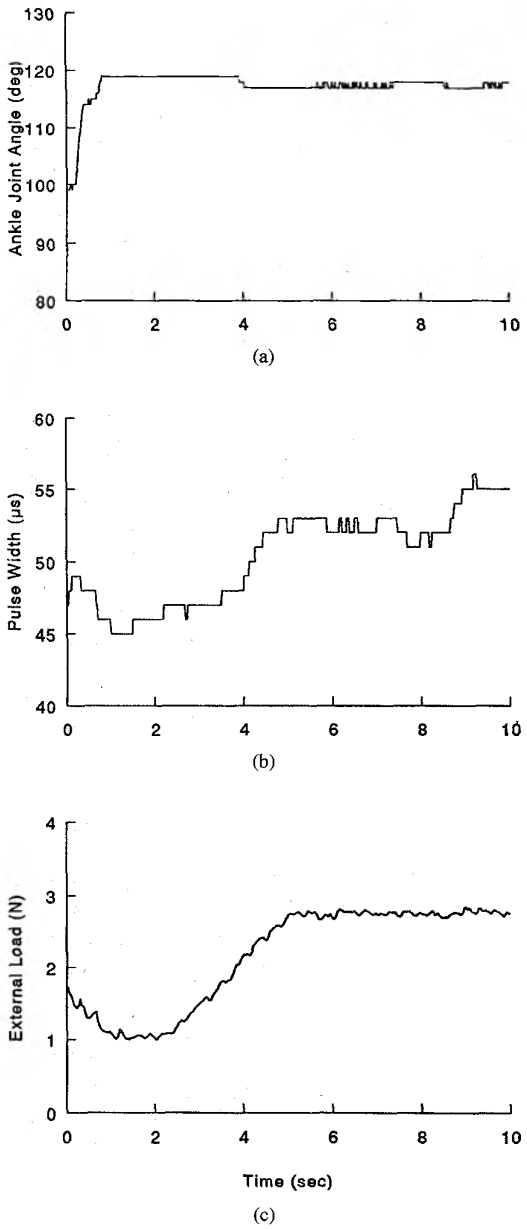

Fig. 4. Example of closed-loop stimulation under a varying external load. (a) Joint angle as a function of time after the controller was given a target position of 117 ° (180 ° = full ankle extension). (b) Pulse width of stimuli delivered to the medial gastrocnemius during this time. (c) The external perturbation force at the footpad.

the largest mean error at the 125° target position. The system was BIBO stable at all target positions.

B. Joint Angle Trajectory Tracking

The joint angle trajectory tracking test was designed to determine the performance limits of the control system for tracking an arbitrary ankle joint trajectory. Fig. 7 illustrates a typical run of this test showing ankle joint tracking of a sinusoidal target trajectory with step increases in trajectory frequency. Trials were also conducted with trajectories with step decreases in trajectory frequency and with constant trajectory frequency. The tracking response was not affected by the order of frequency presentation used.

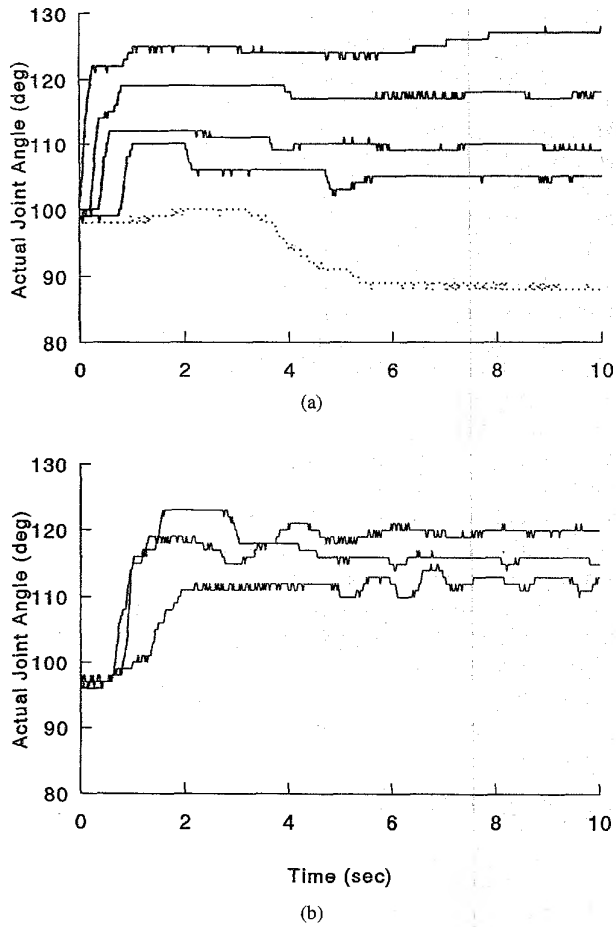

Fig. 5. Example of a joint angle hold test. (a) Measured ankle joint angle as a function of time in response to set target angles of 102°, 110°, 117°, and 125° (solid lines) and in the absence of stimulation (dashed line) in an anesthetized preparation. (b) Results for three target joint angles 110°, 117°, and 125° in an unanesthetized decerebrate preparation. The foot was loaded with an external perturbation force at the footpad that varied with time as shown in Fig. 4(c).

The overall tracking response characteristics were evaluated by determining an average joint angle cycle response for each frequency and amplitude/load condition within an experiment. These average cycle responses were pooled between experiments to determine the overall tracking response of the system for each frequency and amplitude/load condition. The overall tracking responses were fitted to a sinusoid (1) using the Levenberg–Marquardt nonlinear least squares regression [30]

$$y_{fit} = A_1 \sin(\omega t + A_2) + A_3. \quad (1)$$

This least squares fit yielded magnitude, phase, and offset parameters which were used to derive Bode plots for the closed-loop system and the estimator transfer function. The magnitude and phase information from the curve fits for the closed-loop system are plotted in Fig. 8. All four load/range conditions resulted in similar Bode plots with the −3 dB point at about 1 Hz [Fig. 8(a)]. The corresponding phase lag was about −1.25 rad (−72°, [Fig. 8(b)]). These values indicate

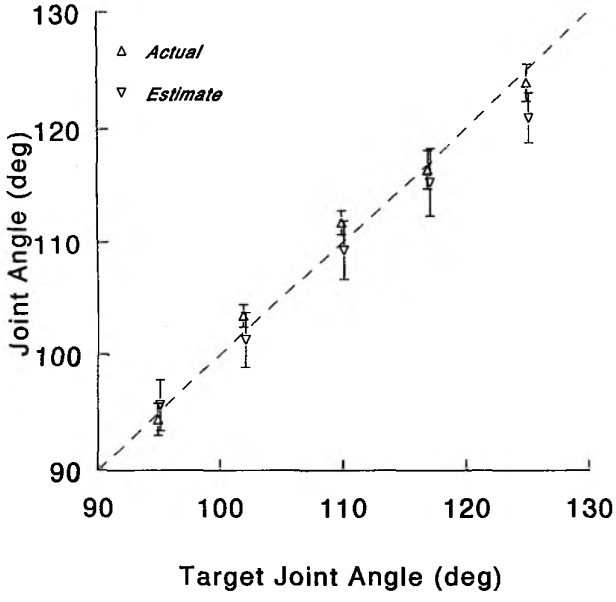

Fig. 6. Steady state joint angle hold performance of the controller. Shown are means ± standard errors ($N = 6$) of the actual and the controller estimates of the joint angles as a function of the target joint angle. Points are slightly displaced laterally for clarity.

that the increase in tracking errors at frequencies above 1 Hz were largely due to phase error.

The joint angle estimator gain plot (Fig. 9) shows that the estimator was not affected by load or trajectory range, but was by the trajectory frequency showing an increase in its gain beginning at about 0.75 Hz. Fig. 9(a) also has points adapted from Matthews [27] showing the gain in single unit muscle spindle sensitivity for comparison. The phase plot of the estimator shows a phase advance beginning at about 0.75 Hz. This is consistent with the behavior of single muscle spindle units described by Matthews [27]. This indicates that increases in the estimator sensitivity are due to increases in the velocity sensitivity of the muscle spindles which were not accounted for in the characterization of the activity to joint angle maps. The breakpoints of the estimator Bode plot, although consistent with that for muscle spindles, are at a slightly lower frequency. The greater increase in sensitivity seen in the results can be partially accounted for by nonlinearities in the tendon moment arms for tibialis anterior and gastrocnemius about the ankle [28] which can lead to faster stretch rates of the muscles in the case of ankle induced stretching compared to direct muscle stretching.

IV. Discussion

The results from the joint angle hold tests indicate that within the physiological range of motion for ankle extension, the controller was able to reach and maintain a target position while compensating for a varying load and muscle fatigue. Near the limits of controllable motion the measured frequency of multiunit activity tended to level off due to an increase in the number of superimposed potentials as the mean interspike interval approached the action potential duration. This limitation could be accommodated by using more selective electrodes, or

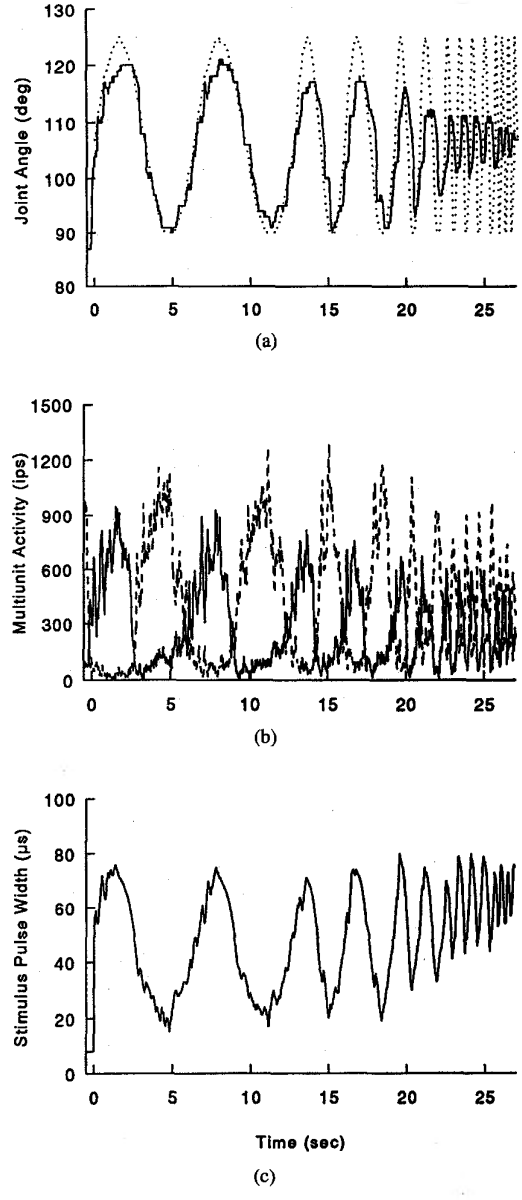

Fig. 7. Typical joint angle tracking run. The condition tested in this run was to track a 35 ° amplitude, sinusoidal trajectory in the presence of a 3-N load. Shown are: (a) The target (dotted line) and actual (solid line) ankle joint angle during the run, (b) the level of recorded activity (impulses per second) from muscle spindle receptors in tibialis anterior (solid line) and lateral gastrocnemius (dashed line), and (c) the controller output.

by setting a higher spike acceptance threshold level for high neural activity levels. The lack of sensitivity at high activity rates probably was the source of the 3° underestimation of joint angle for the 125° target position. However, at this angle the ankle was near its maximum physiological extension, and increases in stimulus duration did not produce further increases in joint angle.

The performance of the controller for the 95° target position was not significantly different than the control run with no stimulation. This is because the rest position of the ankle given an external torque in dorsi-flexion between 7 and 22 N-cm is near this angle. If larger torques were used, the

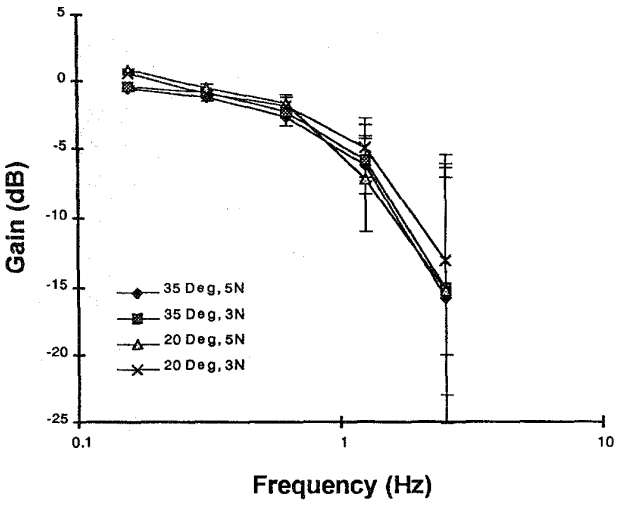

(a)

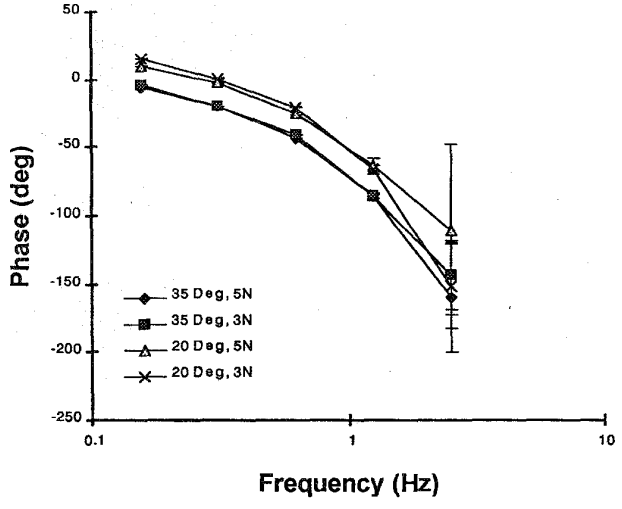

(b)

Fig. 8. Bode plots of the system response to tracking for different stimulus (command signal) amplitudes and loads on the foot. The curves were obtained by fitting the data from the joint angle tracking tests to (1) (see text) using nonlinear least squares regression. Shown are mean ± standard error ($N = 8$) for the system gain (a) and phase (b). The magnitudes were normalized to the amplitude of the target sinusoidal joint angle trajectory. The phases were measured relative to the phase of the target trajectory.

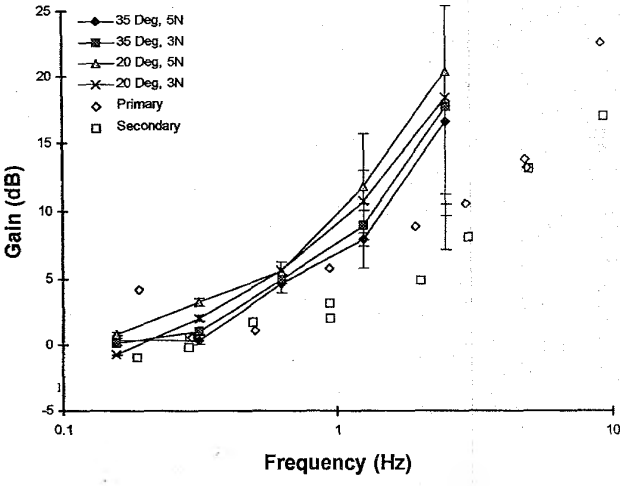

(a)

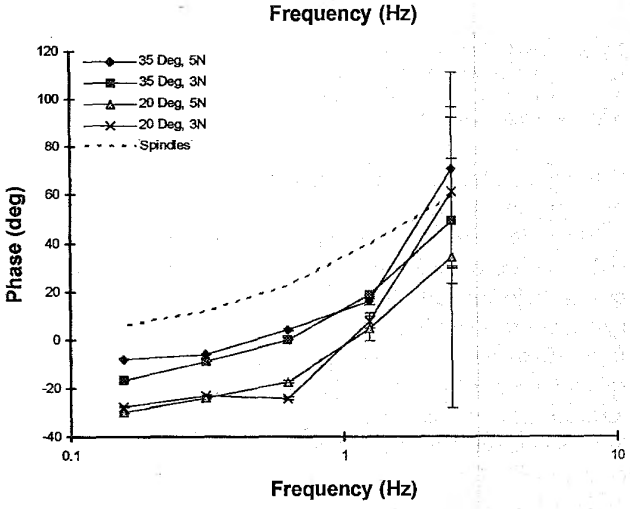

(b)

Fig. 9. Bode plots of the estimator response to four different stimulus (command signal) amplitudes and loads on the foot. Shown are mean ± standard error ($N = 8$) for the estimator gain (a) and phase (b). The magnitudes were normalized to the amplitude of the ankle joint angle trajectory. The phases were measured relative to the phase of the ankle joint trajectory. Plotted for comparison in (a) are points showing the sensitivity gain of primary and secondary muscle spindle single units derived data from Matthews [27]. The broken line shown in (b) corresponds to the phase versus frequency relationship for muscle spindles predicted by Matthews [27].

range of controllable ankle positions would be correspondingly increased.

The joint angle hold test used only feedback from the tibialis anterior muscle spindles. Control of ankle position was achieved since the task only required control in the direction of ankle extension. In cases where the target joint angle positions reversed directions, feedback from a single muscle proved to be ineffective due to the hysteresis in the response of the spindles. To overcome this problem, muscle spindle activity from lateral gastrocnemius was used in addition to that from tibialis anterior.

The results of the joint angle trajectory tracking test indicate that, using feedback from muscle spindles in agonist/antagonist muscle pairs, the system is able to track a sinusoidal joint angle trajectory. The tracking performance was independent of trajectory amplitude and external load. For trajectories cycling at rates less than 1 Hz, the nominal tracking error was 20% of the amplitude, in the range of 4–7°. These errors are similar to the errors seen in the joint angle hold test and are on the order of the linear directionality errors seen for relaxed human subjects [25]. The performance degraded with trajectories that cycled at greater than 1 Hz when muscle phase lag became dominant.

Fig. 9 shows that beginning at about 0.75 Hz the estimator begins to overestimate the magnitude of the joint angle, which

results in errors in joint angle tracking. This overestimation is due to increased sensitivity of the spindles to stretch as a result of dynamic sensitivity in both the primary and secondary spindle endings at frequencies above 1–2 Hz [27], [31]. These increases in dynamic sensitivity occurred for angular velocities greater than 80°/s and thus were not reflected in the activity to joint angle maps. The fastest average transient motions made by the foot during the joint angle hold test to reach a target position were on the order of 30°/s, well below the angular velocity where dynamic spindle sensitivity becomes a significant effect and indicating that the muscle afferent activity was dominated by spindles with static sensitivity.

The nonlinearities of the spindles may help to increase the controllability of the system. Rapid motions towards an overshoot in ankle position are more rapidly detected by the increased dynamic sensitivity of the spindles while rapid motions towards an undershoot are detected by the hysteresis nonlinearity. In both cases, the net result to the system is an increase in negative feedback or muscle stimulation inhibition. This urgency in detecting rapid tracking errors acts to compensate for the relatively slow response of the skeletal muscle actuator. The frequency response of the actuator muscle, medial gastrocnemius, has been reported as having a corner at 2 Hz [32], [33]. Ankle positioning tasks that require motions with angular velocities up to 80°/s would benefit from this feedback scheme.

A more sophisticated feedforward/feedback controller using a model-based estimator that takes into account the frequency response characteristics of muscle activation, the velocity, and the acceleration sensitivities of the spindle organs might improve overall performance of this scheme at higher target trajectory frequencies. The controllable range of the ankle was limited in the present study because only one of the three heads of the triceps surae was used and none of the ankle flexors were stimulated. A controller that used both ankle extensors and flexors would provide control over the full range of motion, but would increase the complexity of the controller.

As with other neural electrodes, it is possible to stimulate and record through the same dLIFE. Although not exploited in the present study, this property could be advantageous in an FNS application to reduce the number of electrodes required. Such a recording/stimulation scheme would require additional hardware or software to blank the amplifier during stimulation and to validate afferent signal samples [34]. Another mode of using intrafascicular electrodes, not utilized in the present experiments, involves separating out single units from the multiunit recording [16], [17], [35]–[37]. These spike separation techniques could be used to monitor the afferent activity from several muscles and cutaneous afferents with a single set of electrodes implanted more proximally in a peripheral nerve.

Multijoint coupling and multiaxis sensitivity of the muscle afferents were not addressed in the present study; however, a combination of the above two recording methods could be used to decouple and resolve individual joints from muscles that act across more than one joint, or have sensitivity in multiple degrees of freedom.

The goal of this study was to determine whether a simple artificial closed-loop control scheme could be used to control a biological system using only natural afferent activity as feedback to the controller. The immediate application of this study is for functional neuromuscular stimulation. The current system, if implemented in a FNS system, may be useful in providing functional control of slow motions such as stance maintenance, transfers, and slow ambulation and provide an alternative to using artificial goniometers.

ACKNOWLEDGMENT

The authors thank T. McNaughton, K. Mirfakhraei, V. Mushahwar, P. R. Burgess, R. Normann, and A. Schoenberg for technical assistance and critical reading of the manuscript.

REFERENCES

[1] P. E. Crago, J. T. Mortimer, and P. H. Peckham, "Closed-loop control of force during electrical stimulation of muscle," *IEEE Trans. Biomed. Eng.*, vol. BME-27, pp. 306–311, 1980.

[2] N. Lan, P. E. Crago, and H. J. Chizeck, "Feedback control methods for task regulation by electrical stimulation of muscles," *IEEE Trans. Biomed. Eng.*, vol. 38, pp. 1213–1223, 1991.

[3] H. J. Chizeck, N. Lan, L. S. Palmieri, and P. E. Crago, "Feedback control of electrically stimulated muscle using simultaneous pulse width and stimulus period modulation," *IEEE Trans. Biomed. Eng.*, vol. 38, pp. 1224–1234, 1991.

[4] D. R. McNeal, R. J. Nakai, P. Meadows, and W. Tu, "Control of the freely-swinging paralyzed leg before and after exercise," in *IX Int. Symp. External Control of Human Extremities,* 1987, pp. 261–273.

[5] R. B. Stein, D. Charles, and K. B. James, "Providing motor control for the handicapped: A fusion of modern neuroscience, bioengineering, and rehabilitation," in *Advances in Neurology,* vol. 47: Functional recovery in neurological disease, pp. 565–581, 1988.

[6] A. Kralj, T. Bajd, R. Turk, J. Krajnik, and H. Benko, "Gait restoration in paraplegic patients: A feasibility demonstration using multichannel surface electrode FES," *J. Rehab. R&D,* vol. 20, pp. 3–20, 1983.

[7] G. R. Cybulski, R. D. Penn, and R. J. Jaeger, "Lower extremity functional neuromuscular stimulation in cases of spinal cord injury," *Neurosurg.*, vol. 15, pp. 132–146, 1984.

[8] A. Prochazka, "Comparison of natural and artificial control of movement," *IEEE Trans. Rehab. Eng.*, vol. 1, pp. 7–16, 1993.

[9] J. T. Mortimer, "Motor prostheses," in *Handbook of Physiology. Section 1: The Nervous System,* Brooks, Ed. Bethesda, MD: Amer. Physiological Soc., 1981, pp. 155–187.

[10] P. E. Crago, R. J. Nakai, and H. J. Chizeck, "Feedback regulation of hand grasp opening and contact force during stimulation of paralyzed muscle," *IEEE Trans. Biomed. Eng.*, vol. 38, pp. 17–28, 1991.

[11] N. Lan, P. E. Crago, and H. J. Chizeck, "Control of end-point forces of a multijoint limb by functional neuromuscular stimulation," *IEEE Trans. Biomed. Eng.*, vol. 38, pp. 953–965, 1991.

[12] J. A. Hoffer and M. K. Haugland, "Signals from tactile sensors in glabrous skin suitable for restoring motor functions in paralyzed humans," in *Neural Prostheses: Replacing Motor Function after Disease or Disability,* Stein and Peckham, Ed. New York: Oxford Univ. Press, 1992, pp. 99–125.

[13] M. K. Haugland, J. A. Hoffer, and T. Sinkjaer, "Skin contact force information in sensory nerve signals recorded by implanted cuff electrodes," *IEEE Trans. Rehab. Eng.*, vol. 2, pp. 18–28, 1994.

[14] M. K. Haugland and J. A. Hoffer, "Slip information provided by nerve cuff signals: Application in closed-loop control of functional electrical stimulation," *IEEE Trans. Rehab. Eng.*, vol. 2, pp. 29–36, 1994.

[15] T. Sinkjaer and M. Haugland, "Cutaneous nerve recordings used for control of FES in man," presented at Neural Prostheses: Motor Systems IV: Engineering Foundation Conf., Deer Creek Resort, OH, 1994.

[16] E. V. Goodall, T. M. Lefurge, and K. W. Horch, "Information contained in sensory nerve recordings made with intrafascicular electrodes," *IEEE Trans. Biomed. Eng.*, vol. 38, pp. 846–850, 1991.

[17] T. G. McNaughton and K. W. Horch, "Action potential classification with dual channel intrafascicular electrodes," *IEEE Trans. Biomed. Eng.*, vol. 41, pp. 609–616, 1994.

[18] N. Nannini and K. Horch, "Muscle recruitment with intrafascicular electrodes," *IEEE Trans. Biomed. Eng.*, vol. 38, pp. 769–776, 1991.

[19] K. Yoshida and K. Horch, "Selective stimulation of peripheral nerve fibers using dual intrafascicular electrodes," *IEEE Trans. Biomed. Eng.*, vol. 40, pp. 492–494, 1993.

[20] ——, "Reduced fatigue in electrically stimulated muscle using dual channel intrafascicular electrodes with interleaved stimulation," *Ann. Biomed. Eng.*, vol. 21, pp. 709–714, 1993.
[21] D. B. Popovic, R. B. Stein, K. L. Jovanovic, R. Dai, A. Kostov, and W. W. Armstrong, "Sensory nerve recording for closed-loop control to restore motor functions," *IEEE Trans. Biomed. Eng.*, vol. 40, pp. 1024–1031, 1993.
[22] J. T. Mortimer, W. F. Agnew, K. Horch, P. Citron, G. Creasey, and C. Kantor, "Perspectives on new electrode technology for stimulating peripheral nerves with implantable motor prostheses," *IEEE Trans. Rehab. Eng.*, vol. 3, pp. 145–153, 1995.
[23] T. Lefurge, E. Goodall, K. Horch, L. Stensaas, and A. Schoenberg, "Chronically implanted intrafascicular recording electrodes," *Ann. Biomed. Eng.*, vol. 19, pp. 197–207, 1991.
[24] R. B. Stein, D. Charles, L. Davis, J. Jhamandas, A. Mannard, and T. R. Nichols, "Principles underlying new methods for chronic neural recording," *Can. J. Neurol. Sci.*, vol. 2, pp. 235–244, 1975.
[25] P. R. Burgess, J. Y. Wei, and F. J. Clark, "Signaling of kinesthetic information by peripheral sensory receptors," *Ann. Rev. Neurosci.*, vol. 5, pp. 171–187, 1982.
[26] J. Y. Wei, B. R. Kripke, and P. R. Burgess, "Joint angle signaling by muscle spindle receptors," *Brain Res.*, vol. 370, pp. 108–118, 1986.
[27] P. B. C. Matthews and R. B. Stein, "The sensitivity of muscle spindle afferents to small sinusoidal changes of length," *J. Physiol.*, vol. 200, pp. 723–743, 1969.
[28] R. P. Young, S. H. Scott, and G. E. Loeb, "An intrinsic mechanism to stabilize posture—joint-angle-dependent moment arms of the feline ankle muscles," *Neurosci. Lett.*, vol. 145, pp. 137–140, 1992.
[29] G. E. Goslow, R. M. Reinking, and D. G. Stuart, "The cat step cycle: Hind limb joint angles and muscle lengths during unrestrained locomotion," *J. Morph.*, vol. 141, pp. 1–42, 1973.
[30] W. H. Press, *Numerical Recipes in C: The Art of Scientific Computing*. Cambridge, U.K.: Cambridge Univ. Press, 1988.
[31] P. B. C. Matthews, "Muscle spindles: their messages and their fusimotor supply," in *Handbook of Physiology. Section 1: The Nervous System*, Brooks, Ed. Bethesda, MD: Amer. Physiological Soc., 1981, pp. 189–228.
[32] R. Baratta and M. Solomonow, "The dynamic response model of nine different skeletal muscles," *IEEE Trans. Biomed. Eng.*, vol. 37, pp. 243–251, 1990.
[33] ——, "The dynamic performance model of skeletal muscle," *Critical Rev. Biomed. Eng.*, vol. 19, pp. 419–454, 1992.
[34] Z. M. Nikolic, D. B. Popovic, R. B. Stein, and Z. Kenwell, "Instrumentation for ENG and EMG recordings in FES systems," *IEEE Trans. Biomed. Eng.*, vol. 41, pp. 703–706, 1994.
[35] E. V. Goodall and K. W. Horch, "Separation of action potentials in multi-unit intrafascicular recordings," *IEEE Trans. Biomed. Eng.*, vol. 39, pp. 289–295, 1992.
[36] E. V. Goodall, K. W. Horch, T. G. McNaughton, and C. M. Lybbert, "Analysis of single-unit firing patterns in multi-unit intrafascicular recordings," *Med. & Biol. Eng. & Comput.*, vol. 31, pp. 257–267, 1993.
[37] K. Mirfakhraei and K. Horch, "Classification of action potentials in multi-unit intrafascicular recordings using neural network pattern recognition techniques.," *IEEE Trans. Biomed. Eng.*, vol. 41, pp. 89–91, 1994.

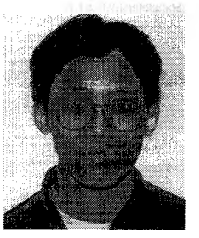

Kenichi Yoshida (S'89–M'91) was born in Los Angeles, CA, in 1965. He received the B.S.E. degree in bioengineering in 1989 from the University of California at Los Angeles and the Ph.D. degree in bioengineering from the University of Utah, Salt Lake City, in 1994.

He is currently a Post Doctoral Fellow in the Division of Neuroscience at the University of Alberta. His research interests include natural sensors, their role in proprioception and motor control, and the application of natural sensors to FNS control schemes.

Dr. Yoshida is a member of Tau Beta Pi.

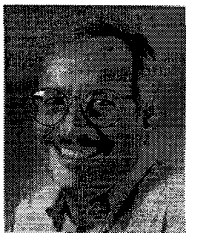

Kenneth W. Horch (M'88) received the B.S. degree from Lehigh University, Bethlehem, PA, and the Ph.D. degree from Yale University, New Haven, CT.

He is currently Professor and Associate Chair of Bioengineering and Professor of Physiology at the University of Utah. His research interests include neuroprosthetics, sensory neurophysiology, motor control bioinstrumentation.